arXiv:2305.19356v1 [hep-ph] 30 May 2023

Twin Pati-Salam theory of flavour for a new picture of B-anomalies

M. Fernández Navarro
School of Physics & Astronomy, University of Southampton, Southampton SO17 1BJ, UK



We discuss a theory of flavour which can simultaneously explain and connect the origin of the Standard Model flavour hierarchies with the $U_1(\mathbf{3},\mathbf{1},2/3)$ leptoquark explanation of the B-decay flavour anomalies. First, we motivate the vector leptoquark U_1 as an excellent mediator to address the updated picture of B-anomalies. Secondly, we introduce the Twin Pati-Salam theory of flavour, which naturally provides a low scale 4321 gauge group with a TeV scale U_1. We show that both the couplings of U_1 to SM fermions and the effective SM Yukawa couplings arise from the same physics, naturally providing a pattern of dominantly left-handed U_1 couplings as most preferred by current data. Finally, we discuss the most promising signals at low energy processes that can test the model in the near future.

1 Introduction

The high number of flavour parameters in the Standard Model (SM) and their suspicious hierarchical pattern might be understood in the form of physics beyond the SM. A well-motivated assumption is that the SM Yukawa couplings arise as effective remnants of a more fundamental theory of flavour, explaining their hierarchical pattern. However, the energy scale Λ of such a theory is commonly unspecified, since theories of flavour usually accommodate the flavour parameters of the SM by fixing the ratios $\langle\phi\rangle/\Lambda$, where ϕ is associated to heavy Higgs bosons spontaneously breaking the gauge structures of the new theory. Nevertheless, such a theory is expected to predict *non-generic* fermion mixing in each charged sector. In absence of a very particular GIM-like suppression, it is possible that the new massive degrees of freedom from the theory of flavour could mediate sizable flavour-changing currents. Given the sensitivity of flavour observables to very high energy scales, we might be able to disentangle the high scales $\langle\phi\rangle$ or Λ from the amount of data obtained in flavour physics experiments.

In this direction, a conspicuous series of anomalies in flavour observables has emerged in the last decade. On the one hand, significant discrepancies between the SM and the experiments in several $b\to s\mu\mu$ observables point to a possible new physics (NP) effect. Nevertheless, such NP must couple similarly to muon and electron pairs in order to pass the lepton flavour universality (LFU) test of the recently updated $R_{K^{(*)}}$ ratios[1]. On the other hand, more discrepancies between the experiment and the SM appear in $b\to c\ell\nu$ charged current transitions, where the remarkable

effect is the possible breaking of LFU suggested by the measurements of the $R_{D^{(*)}}$ ratios, which hint to a preference for the decay $b \to c\tau\nu$ with respect to the transitions involving light charged leptons. Although the measurement of $R_{D^{(*)}}$ is more challenging from the experimental point of view, the world average of current data suggests a departure from the SM at the 3.2σ significance level [1]. All things considered, both sets of anomalies together seem to prefer a sizable new physics effect affecting third family fermions, competing with a tree-level SM charged current, along with a suppressed and flavour universal effect for the light families that explains the neutral current anomalies.

In the following, we will introduce the vector leptoquark $U_1(\mathbf{3}, \mathbf{1}, 2/3)$ as an excellent mediator to address the current picture of anomalies, which moreover is naturally connected to the origin of flavour hierarchies in the SM.

2 The U_1 vector leptoquark and the 4321 embedding

The vector leptoquark $U_1(\mathbf{3}, \mathbf{1}, 2/3)$ contributes at tree-level to the $R_{D^{(*)}}$ ratios via the contact interaction $(\bar{c}_L\gamma^\mu b_L)\,(\bar{\tau}_L\gamma^\mu \nu_L)$. This contribution is also connected to the contact interaction $(\bar{s}_L\gamma^\mu b_L)\,(\bar{\tau}_L\gamma^\mu \tau_L)$ via $SU(2)_L$ invariance. Remarkably, at the 1-loop level the latter provides a contribution to the LFU operator $(\bar{s}_L\gamma^\mu b_L)\,(\bar{\ell}\gamma^\mu \ell)$ [2]. Therefore, a vector leptoquark $U_1(\mathbf{3}, \mathbf{1}, 2/3)$ explaining the $R_{D^{(*)}}$ anomalies naturally delivers a relevant LFU contribution to $b \to s\ell\ell$ that can reduce the tension with the experiment.

Nevertheless, the explanation of the $R_{D^{(*)}}$ anomalies requires a TeV scale U_1. Such a light vector leptoquark arising from traditional Pati-Salam (PS) embeddings would be at odds with data from flavour-violating kaon decays. However, model building efforts in recent years led to the so-called "4321" gauge group [3] (for alternative constructions see e.g. [2]):

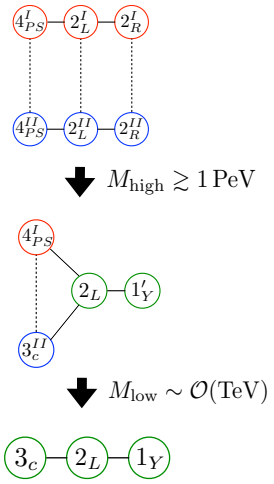
$$SU(4) \times SU(3)' \times SU(2)_L \times U(1)_{Y'}\,, \tag{1}$$

which can provide a TeV scale U_1 as long as the first and second fermion families are singlets under $SU(4)$. The theory further predicts a heavy Z' and coloron g' with masses in the TeV ballpark as well, plus heavy vector-like (VL) fermions that induce U_1 couplings to the light families through mixing.

In recent years, several theories of flavour have been proposed assuming that the third SM family transforms non-trivially under $SU(4)$, see e.g. [4]. However, all of them predict a sizable coupling of third family right-handed (RH) fermions to U_1, which is tightly constrained by direct searches at LHC, see e.g. the recent review [5]. Instead, if the third family is a singlet under $SU(4)$, then the U_1 currents can be dominantly left-handed (LH), a scenario compatible with current high energy data. In this so-called "fermiophobic" scenario, the couplings of U_1 to SM fermions are all induced through mixing with vector-like fermions that transform non-trivially under $SU(4)$. Nevertheless, the flavour structure of such a model is ad-hoc, worsening the flavour puzzle with a bunch of extra parameters that give no information about the origin of flavour in the SM. We will show in the following a theory of flavour featuring a low scale fermiophobic 4321 model, which addresses the origin of flavour hierarchies in the SM and predicts an even richer phenomenology.

3 The Twin Pati-Salam theory of flavour

Given the structure of the fermiophobic 4321 group described in the previous section, where a set of vector-like fermions transforms under $SU(4)$ while SM-like fermions transform under $SU(3)'$, a natural UV completion would be that of two commuting Pati-Salam groups, one for vector-like fermions and another one for SM-like fermions. This is the basic structure of the *Twin Pati-Salam* gauge group [6,7] introduced in Fig. 1, which includes a scalar sector linking both PS sites.



(a)

Field	$SU(4)^I_{PS}$	$SU(2)^I_L$	$SU(2)^I_R$	$SU(4)^{II}_{PS}$	$SU(2)^{II}_L$	$SU(2)^{II}_R$
$\Psi_{L(1,2,3)}$	**1**	**1**	**1**	**4**	**2**	**1**
$\psi_{R(1,2,3)}$	**1**	**1**	**1**	**4**	**1**	**2**
$\Psi_{L(4,5,6)}$	**4**	**2**	**1**	**1**	**1**	**1**
$\tilde{\Psi}_{R(4,5,6)}$	**4**	**2**	**1**	**1**	**1**	**1**
$\tilde{\psi}_{L(4,5,6}$	**4**	**1**	**2**	**1**	**1**	**1**
$\psi_{R(4,5,6)}$	**4**	**1**	**2**	**1**	**1**	**1**
ϕ	$\overline{\mathbf{4}}$	$\overline{\mathbf{2}}$	**1**	**4**	**2**	**1**
$\bar{\phi}$	**4**	**1**	**2**	$\overline{\mathbf{4}}$	**1**	$\overline{\mathbf{2}}$
H	**4**	**2**	**1**	$\overline{\mathbf{4}}$	**1**	$\overline{\mathbf{2}}$
$\bar{H}$	$\overline{\mathbf{4}}$	**1**	$\overline{\mathbf{2}}$	**4**	**2**	**1**
Ω_{15}	**15**	**1**	**1**	**1**	**1**	**1**

(b)

Figure 1: The model is based on two copies of the PS gauge group $SU(4)_{PS} \times SU(2)_L \times SU(2)_R$. The circles represent the gauge groups with the indicated symmetry breaking. Three families of SM-like (chiral) fermions, arranged in Pati-Salam multiplets, transform under PS^{II} (in blue), while three families of vector-like fermions (denoted 4, 5 and 6) transform under PS^{I} (in red). The Twin Pati-Salam symmetry is spontaneously broken down to the 4321 group at high energies $M_{\rm High} \gtrsim 1\,{\rm PeV}$ (via scalar content not shown here, we refer the reader to [6,7]), then the 4321 group is broken to the SM at the scale $M_{\rm low} \sim \mathcal{O}({\rm TeV})$ (via the scalars ϕ and $\bar{\phi}$ connecting both PS groups). The Higgs H and $\bar{H}$ decompose in a multi-Higgs doublet model at low energies and perform electroweak symmetry breaking, see [6,7].

3.1 Effective Yukawa and U_1 couplings

The scalar sector of the model is chosen such that renormalisable Yukawa couplings for SM-like fermions are forbidden. Nevertheless, the scalar sector acts as a link between the two PS groups, generating mixing between vector-like and SM-like fermions which provides effective Yukawa couplings and effective U_1 couplings for SM-like fermions [a]. In Fig. 2 we display this mechanism at work. The third family effective Yukawa couplings are connected to the ratio of the TeV scale VEVs of the scalars ϕ_3 and ϕ_1 over the mass of $SU(2)_L$ doublet fourth family vector-like fermions $M_4^{Q,L}$. The effective U_1 couplings to third family fermions arise from this mixing as well, so they are connected to the same ratios of NP scales. As an example, we include below the effective top Yukawa and LH third family U_1 coupling as

$$y_t \sim \frac{\langle \phi_3 \rangle}{M_4^Q} \sim \mathcal{O}(1) \Longrightarrow \beta^L_{Q_3 L_3} \sim \frac{\langle \phi_3 \rangle}{M_4^Q} \frac{\langle \phi_1 \rangle}{M_4^L} \sim \mathcal{O}(1)\,, \tag{2}$$

where the ratio $\langle \phi_1 \rangle / M_4^L$ is also expected to be $\mathcal{O}(1)$ since the twin PS symmetry enforces $M_4^Q \sim M_4^L$. Therefore, the prediction of an $\mathcal{O}(1)$ top Yukawa coupling leads to an $\mathcal{O}(1)$ third family LH coupling to U_1 as well. In contrast, the effective Yukawa couplings for second family fermions arise from mixing with $SU(2)_L$ singlet fourth family vector-like fermions. As a consequence, they are connected to ratios of the VEVs of other scalars $\bar{\phi}_3$ and $\bar{\phi}_1$ (whose VEVs are also TeV scale since they also participate in 4321 spontaneous breaking) over the mass of the $SU(2)_L$ singlet vector-like fermions $M_4^{u,d,e}$. This mixing leads to suppressed U_1 couplings to RH SM-like

[a] In the simplified model discussed here, we work in the first family massless approximation (since only second and thid family fermions are relevant for our description of the B-anomalies) and we do not discuss the extended Higgs sector of the model. We refer the interested reader to [6,7] where the complete model is presented and discussed.

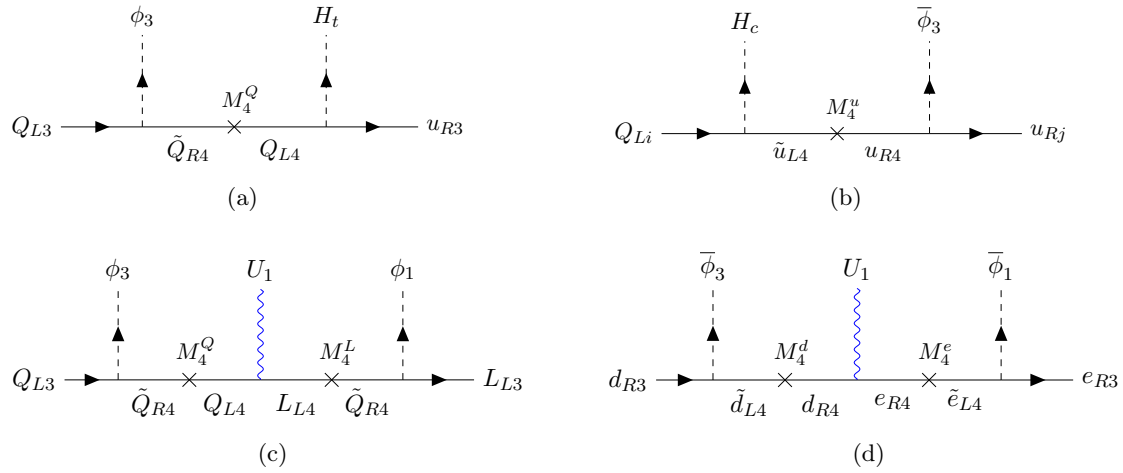


Figure 2: ***(Top)*** Diagrams leading to effective Yukawa couplings for the top quark (left), charm quark and their mixing (right), with $i, j = 2, 3$ ***(Bottom)*** Diagrams leading to effective U_1 couplings to third family LH fermions (left) and RH fermions (right).

fermions, since they are connected to the origin of second family fermion masses,

$$y_c \sim \frac{\langle \bar{\phi}_3 \rangle}{M_4^u} \ll 1 \Rightarrow \beta^R_{b\tau} \sim \frac{\langle \bar{\phi}_3 \rangle}{M_4^d} \frac{\langle \bar{\phi}_1 \rangle}{M_4^e} \ll 1\,, \tag{3}$$

where again the Twin PS symmetry enforces $M_4^u \sim M_4^d \sim M_4^e$. This way, just by predicting flavour hierarchies we obtain the desired pattern of *dominantly left-handed* U_1 couplings. Remarkably, the $SU(2)_L$ doublet fermions in the fourth family have to live at the TeV scale in order to explain the fermion masses and U_1 couplings, within the reach of LHC. Instead, the $SU(2)_L$ singlet fourth family vector-like fermions are expected to be much heavier in order to explain the lighter second family fermions.

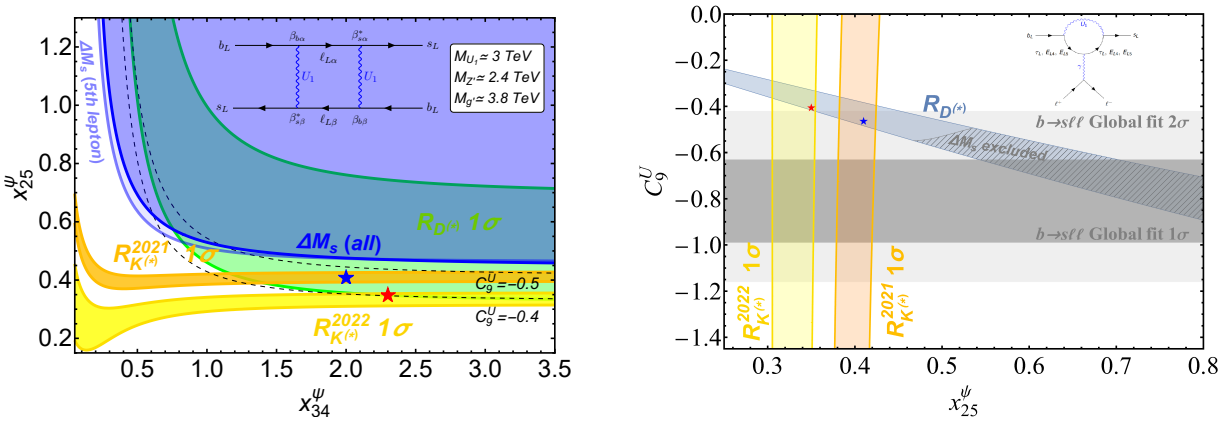
3.2 GIM-like mechanism at work

In the previous section we have introduced how large and dominantly LH couplings for third family fermions arise in the model, while couplings to RH fermions are naturally suppressed. So far, only the fourth family vector-like fermions have been introduced. From now on, we shall assume that another (fifth) family of vector-like fermions mixes with the fourth family, while a sixth family remains unmixed. This mixing is different between the quark and lepton sector (thanks to the Ω_{15} scalar), the particular mechanism explained in detail in Ref. [7]. Such a pattern of VL fermion mixing predicts a CKM-like matrix for the U_1 interactions with VL fermions,

$$\mathcal{L}_{U_1} = \frac{g_4}{\sqrt{2}} \begin{pmatrix} \overline{Q}_{L4} & \overline{Q}_{L5} & \overline{Q}_{L6} \end{pmatrix} \gamma_\mu \begin{pmatrix} c_{\theta_{LQ}} & -s_{\theta_{LQ}} & 0 \\ s_{\theta_{LQ}} & c_{\theta_{LQ}} & 0 \\ 0 & 0 & 1 \end{pmatrix} \begin{pmatrix} L_{L4} \\ L_{L5} \\ L_{L6} \end{pmatrix} U_1^\mu + \text{h.c.} \tag{4}$$

The CKM-like matrix above, containing the $s_{\theta_{LQ}}$ mixing, cancels for the neutral currents mediated by the Z' and g', which at this point remain flavour universal in vector-like fermion flavour space. Now we introduce the 3-4 mixing discussed in the previous section, plus 2-5 and 1-6 fermion mixing in a similar manner, obtaining

$$\mathcal{L}_{U_1} = \frac{g_4}{\sqrt{2}} \begin{pmatrix} \overline{Q}_{L1} & \overline{Q}_{L2} & \overline{Q}_{L3} \end{pmatrix} \gamma_\mu \begin{pmatrix} s^Q_{16} s^Q_{26} & 0 & 0 \\ 0 & c_{\theta_{LQ}} s^Q_{25} s^Q_{25} & s_{\theta_{LQ}} s^Q_{25} s^L_{34} \\ 0 & -s_{\theta_{LQ}} s^Q_{34} s^L_{25} & c_{\theta_{LQ}} s^Q_{34} s^Q_{34} \end{pmatrix} \begin{pmatrix} L_{L1} \\ L_{L2} \\ L_{L3} \end{pmatrix} U_1^\mu + \text{h.c.} \tag{5}$$



(a) (b)

Figure 3: ***(Left)*** Parameter space in the plane $(x^\psi_{34}, x^\psi_{25})$ compatible with $R_{D^{(*)}}$ and $R_{K^{(*)}}$ at 1σ, with the remaining parameters are fixed as in the benchmark of [7]. The blue region is excluded at 95% CL by ΔM_s. ***(Right)*** C_9^U as a function of x^ψ_{25}. Regions preferred by the B-anomalies are depicted. Data for the global fit to $b \to s\ell\ell$ is taken from [8].

where one can now read the relevant couplings participating in the B-anomalies as

$$\left.\begin{aligned} \beta^L_{b\tau} &= c_{\theta_{LQ}} s^Q_{34} s^L_{34} \\ \beta^L_{s\tau} &= s_{\theta_{LQ}} s^Q_{25} s^L_{34} \approx \beta_{c\nu_\tau} \end{aligned}\right\} \Rightarrow \delta R_{D^{(*)}} = \frac{R_{D^{(*)}}}{R^{\rm SM}_{D^{(*)}}} \propto \beta^L_{b\tau}\beta^L_{s\tau}\,, \tag{6}$$

where a value $s_{\theta_{LQ}} \approx 1/\sqrt{2}$ allows for the largest contribution to $\delta R_{D^{(*)}}$, and provides $\beta^L_{b\tau} \approx 1/\sqrt{2}$. The fact that $\beta^L_{b\tau}$ is smaller than 1 ameliorates constraints from direct searches at LHC and LFU tests of τ decays. Remarkably, the model predicts $\delta R_D = \delta R_{D^*}$.

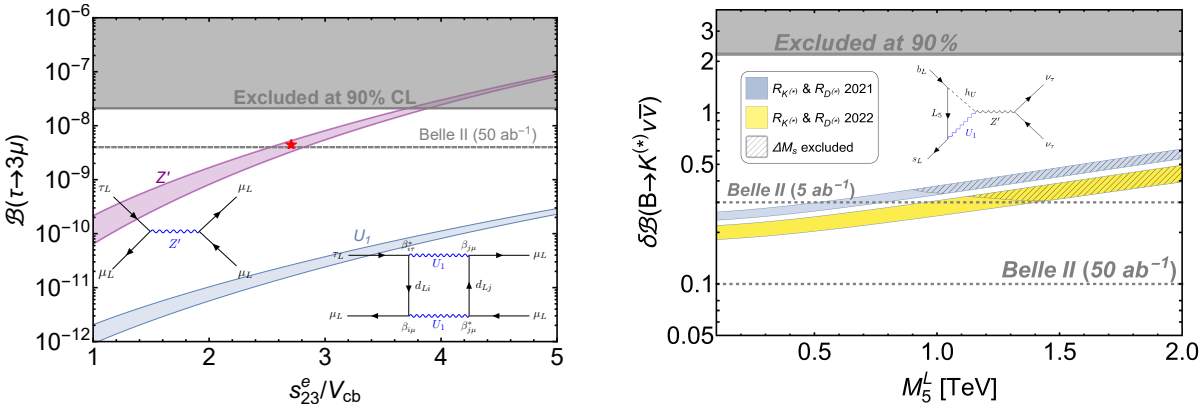
In the basis of Eq. 5, the neutral currents mediated by the Z' and g' become flavour diagonal (up to CKM and lepton mixing). Enforcing $s^Q_{34} = s^Q_{25} = s^Q_{16}$ would suppress all FCNCs, but given the large mixing angles $s^{Q,L}_{34} \approx 1$ required to explain the heaviness of the top, this condition would lead to unsuppressed coloron production at the LHC. Instead, we can enforce $s^Q_{34} = s^Q_{25}$, which protects from the most dangerous FCNCs but allows sizable 2-3 transitions.

4 Low energy phenomenology

Having introduced the model and fixed all the different NP scales in the previous section, now we explore the parameter space of $s^{Q,L}_{34} \propto x^\psi_{34}$ and $s^{Q,L}_{25} \propto x^\psi_{25}$, where x^ψ_{34} and x^ψ_{25} are the dimensionless couplings that control VL-SM fermion mixing. As depicted in Fig. 3a, the model can accommodate the $R_{D^{(*)}}$ anomalies within the 1σ region preferred by the experiment. We highlight the regions preferred by $R_{K^{(*)}}$ according to the 2021 and 2022 measurements, respectively. A large contribution to the mass difference ΔM_s from $B_s - \bar{B}_s$ meson mixing arises in our model at 1-loop, mediated by U_1. Nevertheless, this constraint is relaxed if vector-like fermions running in the loop are lighter than 1 TeV, giving a clear prediction for direct searches at LHC.

In Fig. 3b, we depict the values of the Wilson coefficient C_9^U associated to the LFU operator $(\bar{s}_L\gamma^\mu b_L)\,(\bar{\ell}\gamma^\mu\ell)$ that are preferred by $R_{D^{(*)}}$ and $R_{K^{(*)}}$. Due to the correlations with $R_{K^{(*)}}$, the model can deliver $C_9^U \approx -0.4$, which is close to the values preferred at 2σ by the global fit [8].

Furthermore, the model predicts a sizable enhancement of several observables above their SM prediction. In Fig. 4a, we highlight the enhancement of $\tau \to 3\mu$ mediated by the heavy Z' boson. This signal is connected to non-generic $\mu - \tau$ mixing predicted by the Twin PS theory of flavour, being a consequence of the mechanism explaining flavour hierarchies. In Fig. 4b, we highlight



(a) (b)

Figure 4: ***(Left)*** $\mathcal{B}(\tau \to 3\mu)$ as a function of the $\mu-\tau$ mixing sine s^e_{23}. The purple region denotes the Z' contribution while the blue region denotes the U_1 contribution. ***(Right)*** $\delta(B \to K\bar{\nu}\nu) = \mathcal{B}(B \to K\bar{\nu}\nu)/\mathcal{B}(B \to K\bar{\nu}\nu)_{\rm SM} - 1$ as a function of the 5th family vector-like mass term.

the enhancement of $B \to K^{(*)}\bar{\nu}\nu$ over the SM prediction, which is within the future reach of the Belle II collaboration. Remarkably, given the dominantly LH nature of U_1 couplings in the Twin PS model, this signal is much more enhanced with respect to alternative constructions [4].

5 Conclusions

The Twin Pati-Salam theory of flavour naturally predicts a TeV scale $U_1(\mathbf{3},\mathbf{1},2/3)$ leptoquark with the proper features to address the current picture of B-anomalies, and connects the origin of the U_1 couplings to SM fermions with the origin of effective Yukawa couplings in the SM. A relevant enhancement of key low energy observables will allow to test the model in the near future, along with a rich spectrum of gauge bosons and vector-like fermions at the TeV scale.

Acknowledgments

I thank my collaborator Steve King and I thank Xavier Ponce Díaz for support during the preparation of my talk and valuable comments about my slides. I am very grateful to the organisers of the Moriond conference, and in particular to Jean-Marie Frère, for the inspiring atmosphere during the conference, for the kind invitation and for trusting me for a plenary talk at such an early stage of my career. This work has received funding from the European Union's Horizon 2020 Research and Innovation Programme under Marie Skłodowska-Curie grant agreement HIDDeN European ITN project (H2020-MSCA-ITN-2019//860881-HIDDeN).

References

1. LHCb. *LHCb-PAPER-2022-046*. A. Mathad. *Talk at Rencontres de Moriond EW, 2023.*
2. A. Crivellin et al. *Phys. Rev. Lett.*, 122(1):011805, 2019. L. Calibbi et al. *Phys. Rev. D*, 98(11):115002, 2018. M. Blanke et al. *Phys. Rev. Lett.*, 121(1):011801, 2018.
3. L. Di Luzio, A. Greljo, and M. Nardecchia. *Phys. Rev. D*, 96(11):115011, 2017.
4. M. Bordone et al. *Phys.Lett.B*, 779:317–323, 2018. J. Davighi et al. *JHEP*, 04:030, 2023. Fuentes-Martin et al. *Phys. Lett. B*, 834:137382, 2022.
5. J. Aebischer et al. *Eur. Phys. J. C*, 83(2):153, 2023.
6. S. F. King. *JHEP*, 11:161, 2021.
7. M. Fernández Navarro and S. F. King. *JHEP*, 02:188, 2023.
8. M. Algueró et al. *Eur. Phys. J. C*, 82(4):326, 2022.